NASA MEMO 4-12-59L

NASA MEMO 4-12-59L

NASA

MEMORANDUM

EXPERIMENTAL INVESTIGATION OF EFFECTS OF RANDOM LOADING ON THE FATIGUE LIFE OF NOTCHED CANTILEVER-BEAM SPECIMENS OF 7075-T6 ALUMINUM ALLOY

By Robert W. Fralich

Langley Research Center
Langley Field, Va.

NATIONAL AERONAUTICS AND SPACE ADMINISTRATION
WASHINGTON
June 1959

NATIONAL AERONAUTICS AND SPACE ADMINISTRATION

MEMORANDUM 4-12-59L

EXPERIMENTAL INVESTIGATION OF EFFECTS OF RANDOM LOADING ON THE FATIGUE LIFE OF NOTCHED CANTILEVER-BEAM SPECIMENS OF 7075-T6 ALUMINUM ALLOY

By Robert W. Fralich

SUMMARY

Results of random-loading fatigue tests on 125 notched cantilever-beam specimens and constant-amplitude fatigue tests on 46 similar specimens are presented in terms of the root-mean-square value of peak stresses. The results from the two sets of tests are compared on the basis of time to failure, where the results from the constant-amplitude tests are expressed in terms of an equivalent time to failure based on the natural period of vibration. Compared on this basis, failure at the lower stress levels occurred in a shorter time for the random loading than for the constant-amplitude loading, whereas at the higher stress levels failure occurred in the reverse order. A theoretical result for random loading is also presented and compared with the experimental results. The theoretical result shows good agreement with experiment for low values of stress but underestimates the time to failure at the higher stresses.

INTRODUCTION

One of the problems encountered in aircraft today is the fatigue failure of structural components subjected to random loadings. Examples of random loadings are gust loads, buffeting loads, runway-roughness loads, and acoustic pressure loads in the noise fields of jet and rocket engines. All such loads are characterized by a continuous frequency spectrum over a wide range of frequencies; the shape and magnitude of the spectrum may be different for each of these loadings. (See, for example, refs. 1 to 5.)

Application of a random load to a structure produces a dynamic response which depends on the characteristics of the structure as well as on the loads. The stress histories produced in the structure may consist of a repetition of stress peaks of sufficient magnitude to cause fatigue damage. There is particular danger of fatigue failure if the

structural characteristics are such that a natural frequency occurs in a region where the loading spectrum has appreciable magnitude.

In the past, most fatigue investigations have dealt with the application of loads of constant amplitude rather than with random loads. In order to investigate and compare fatigue properties under the two types of loading, an experimental investigation using 7075-T6 aluminum-alloy specimens was made. These specimens were notched cantilever beams and were tested by applying the load laterally at the tip. Some of the results of the present investigation were included in reference 6. The purpose of the present paper is to present the complete set of experimental results and to describe the testing apparatus and procedure. Also presented is a calculated theoretical result for random loading based on the method of reference 7.

SYMBOLS

f	frequency, cps
f_o	resonant frequency, cps
$N(\sigma)$	number of cycles to failure for stress reversals with amplitude of σ
$P_m(\sigma)$	probability density of stress reversals
R	root radius, in.
T_f	time to failure, sec
$w_\sigma(f)$	power spectral density of stress
σ	stress, ksi or psi
$\sqrt{\overline{\sigma^2}}$	root-mean-square stress, ksi or psi
$\sqrt{\overline{\sigma_p{}^2}}$	root mean square of peak stress, ksi

EXPERIMENTAL INVESTIGATION

Specimens

The specimen configuration used in this investigation is shown in figure 1. Notched specimens were used to utilize the effect of stress concentration in attaining effective stress levels of sufficient magnitude to carry out the fatigue tests in a reasonable length of time with the equipment available. These specimens were machined from 1/4-inch 7075-T6 aluminum plate free from scratches; no special polishing was used. The cantilever specimens had an unclamped length of 3 inches, a width of 1 inch, and two 60° notches located $2\frac{1}{2}$ inches from the tip. The notches were 5/16 inch deep with a root radius R of 0.005 ± 0.001 inch. The dimensions shown in figure 1 are nominal; the actual dimensions used for computing section properties were measured for each specimen to the nearest 0.001 inch before testing.

Test Equipment

Random loading tests.- The equipment used in the random-loading fatigue tests applied the desired force to the specimen, measured and recorded the force and strain data, and indicated the time of fatigue failure. A schematic diagram of this equipment is shown in figure 2 and an overall view of the test equipment is presented in figure 3.

The random force applied in these tests was obtained from a tape recording of repetitions of a 6.4-second sample of the noise produced by a 2-inch subsonic cold air jet. Although this type of random-force signal was used for these tests, an equivalent power spectrum of stress response could have been obtained from other types of random-force inputs provided that they had comparatively flat spectra in the vicinity of the natural frequency of the specimen and no large peaks in the other frequency ranges.

In the equipment shown in figure 2(a), a magnetic tape recorder was used to play back the force signal. The recording of the force signal was frequency modulated so that wear of the magnetic tape during testing would not affect the magnitude of the force signal. A discriminator was used to demodulate the force signal, and a 500-cps low-pass filter was used to remove any high-frequency components traceable to the frequency-modulated carrier frequency. Next, the signal passed through two stages of amplification and then was fed into an 8-pound vector-force electromagnetic shaker which applied the load to the specimen. A timer was also included in this circuit to measure the time to failure.

Because it was impossible to obtain accurate matching of impedance between the shaker and amplifier for all frequency components of the force signal between 0 and 500 cps, it was necessary to use an oversized amplifier (500 watts) to drive the shaker without undue distortion. The moving element of the shaker had a weight of 0.86 pound and a maximum travel of ±1/4 inch.

Each specimen was clamped in support blocks between plastic shims which were inserted to relieve effects of stress concentration at the root. (See figs. 1 and 4.) The shaker drive coil was connected to the tip of the specimen by a flexible connector which eliminated torsional and longitudinal loads. (See fig. 4.) The fundamental natural frequency of the specimen with the shaker attached was about 119 cps.

The equipment shown in figure 2(b) was used to measure and record the current in the shaker drive coil (proportional to the force applied to the shaker drive coil) and the output of a strain gage mounted on the specimen. These force and strain signals were amplified and read on a root-mean-square thermocouple meter and also recorded on magnetic tape. Provision was also made to apply a known calibration signal to the meter and the tape recorder. A cathode-ray oscillograph was used to monitor the force and strain signals.

A failure-detection circuit was also included in the testing apparatus. In this circuit, the breaking of a crack-detecting wire cemented to the specimen actuated a relay which turned off the power to all equipment. Provision was also made to bypass the relay so that the equipment could be operated without crack-detector wires if so desired.

Constant-amplitude-loading tests.- For the part of the experimental investigation with constant-amplitude loading, bending tests were carried out in the fatigue machine shown in figure 5. In this machine, a sinusoidal force was produced by an unbalanced rotating mass which rotated at a constant speed of 1,800 rpm. The machine had a counter which recorded the number of stress cycles applied and a switch that turned the machine off upon specimen failure. Each specimen was mounted as shown in figure 6. As in the previous tests, plastic shims were used at the root, and the machine attachment allowed only lateral forces to be applied at the tip. The root-mean-square value of stress in the specimen was measured with the same equipment (fig. 2(b)) described for the random-loading tests. The stress could also be obtained from the calibrated eccentricity of the rotating weight. This latter method was used for several specimens when strain gages were not applied.

Calculation of Stresses From Measured Strains

The stress in each specimen was obtained from the output of a wire-resistance strain gage mounted at the notched section of the specimen.

(See fig. 1.) Inasmuch as the magnitude of the stress varied over the area covered by the strain gage, the output of the strain gage gave an average of the strain in the region of the notched section. In order to find the relationship between the nominal stress at the notched section and the output of the strain-gage bridge, the specimen was mounted in a test fixture similar to that used in the fatigue tests, and a given static load was applied at the tip. The strain-gage-bridge output in volts was used in conjunction with the calculated surface-bending stress at the notched cross section to obtain a stress-calibration factor. The calculated stress was based on beam properties at the notch, and the effect of stress concentration was neglected. For the fatigue tests, the stress calibration factor was used to obtain root-mean-square values of nominal stress from the measured root-mean-square value of the bridge output.

Test Procedure and Results

Random loading tests.- In this investigation, 125 specimens were tested to failure at zero mean stress and various levels of root-mean-square stress. At the start of the test on each specimen, the root-mean-square value of force was adjusted to give the desired root-mean-square value of stress and was held constant during the remainder of the test. As soon as possible after the test was started, a 45-second sample of each of the signals was recorded on magnetic tape. The test was continued until complete failure of the specimen took place. The time to failure was then recorded.

The characteristics of the force input and stress output are shown in figure 7. Two-second records of the force and stress time histories are shown in figure 7(a) for a specimen tested at a root-mean-square stress of 5,740 psi. The force shown in this figure is the input force applied to the vibrating system; that is, the force applied at the shaker drive coil. The corresponding power spectra are shown in figure 7(b) for the force signal and in 7(c) for the stress signal; the magnitudes are given on logarithmic vertical scales. The stress spectrum shown in figure 7(c) indicates that the vibrating system was lightly damped.

In order to check the probability distribution of the stress, an electronic counter was used to count the number of times in 10 seconds that the stress would cross various levels with positive slope. For example, the results for a specimen with a root-mean-square stress of 4,330 psi are given by the test points of figure 8. Each test point represents the average of five readings and gives the average number of times per second that the stress passes through the value given by the abscissa with positive slope. The solid curve, based on a Gaussian process for a lightly damped system, shows the expected number of times per second that the stress will pass through a given value with positive slope. For the experimental results, the average number of crossings

per second with positive slope are seen to be nearly the same as the expected number of crossings per second with positive slope for a Gaussian distribution of stress; therefore, the probability distribution of the stress for the experimental results was considered to be nearly Gaussian.

The results of the 125 random-loading tests are given in figure 9 in terms of the quantities measured in the tests, that is, the root-mean-square nominal stress and the time to failure. Also shown on this figure is a curve drawn through the average values of the test results. Note that the test points shown here have less scatter than is usual for most fatigue test results.

Constant-amplitude-loading tests.- Constant-amplitude-loading tests were made on 46 specimens at various stress amplitudes and zero mean stress. Before the test on each specimen was started, the amount of eccentricity of the rotating weight in the testing machine was adjusted to give the desired stress level. The fatigue results for the 46 specimens are presented in figure 10 in which the number of stress reversals for failure is shown as a function of stress amplitude. Also shown is a curve drawn through the average values of the test results. The test data were limited to the capacity of the testing machine; however, information at the higher stress levels was desirable for use in theoretical calculations. Consequently, the dashed part of the curve of figure 10 represents an extrapolation based on fatigue results of other notched specimens of similar material.

THEORETICAL CALCULATION

A theoretical calculation of the probable time to failure for a random type of loading is based on a theory given in reference 7. In this theory, based on Miner's rule for cumulative fatigue damage (ref. 8), the time to failure T_f in seconds is given by:

$$T_f = \left[\int_0^\infty \frac{P_m(\sigma)d\sigma}{N(\sigma)}\right]^{-1} \tag{1}$$

where $N(\sigma)$ is the number of cycles to failure for stress reversals with an amplitude σ, and $P_m(\sigma)d\sigma$ is the probable number of stress reversals per second with amplitudes between σ and $\sigma + d\sigma$.

In reference 7, the assumption was made that $P_m(\sigma)d\sigma$, for a Gaussian probability distribution, is equal to the number of peaks per second with amplitudes between σ and $\sigma + d\sigma$. The expression for $P_m(\sigma)$ then becomes

$$P_m(\sigma) = \frac{1}{2\pi\psi_o}\left(-\frac{1}{\psi_o''}\sqrt{\frac{M}{2\pi}}\,e^{\frac{\psi_o''\psi_o''''\sigma^2}{2M}} + \frac{1}{2}\sqrt{-\frac{\psi_o''}{\psi_o}}\,\sigma e^{-\frac{\sigma^2}{2\psi_o}}\left\{1 + \operatorname{erf}\left[\frac{(\psi_o'')^2\sigma}{\sqrt{-2\psi_o\psi_o''M}}\right]\right\}\right) \tag{2}$$

where

$$M = -\psi_o''\left[\psi_o\psi_o'''' - (\psi_o'')^2\right]$$

and

$$\left.\begin{aligned}\psi_o &= \int_0^\infty w_\sigma(f)df = \overline{\sigma^2}\\ \psi_o'' &= -4\pi^2\int_0^\infty f^2 w_\sigma(f)df\\ \psi_o'''' &= 16\pi^4\int_0^\infty f^4 w_\sigma(f)df\end{aligned}\right\} \tag{3}$$

in which $w_\sigma(f)$ is the power spectral density of stress, f is frequency, and $\overline{\sigma^2}$ is the mean square stress.

Equation (1), upon substitution of equation (2) for $P_m(\sigma)$ and of the values of $N(\sigma)$ from fatigue data for the material, can be integrated to obtain the probable time to failure as a function of the root-mean-square stress. However, since fatigue life for constant-amplitude tests is generally considered to depend upon stress amplitudes rather than upon the shape of the stress time history, it is desirable to express the probable time to failure in terms of the root-mean-square value of the peak stresses rather than the root-mean-square stress. It can be shown that for a Gaussian probability distribution, the relationship between the root-mean-square value of the peak stresses $\sqrt{\overline{\sigma_p^2}}$ and the root-mean-square stress $\sqrt{\overline{\sigma^2}}$ is given by

$$\sqrt{\overline{\sigma_p^2}} = \left(\frac{\int_{-\infty}^{\infty} \sigma^2 P_m \, d\sigma}{\int_{-\infty}^{\infty} P_m \, d\sigma} \right)^{1/2} = \left[\psi_o + \frac{(\psi_o'')^2}{\psi_o''''} \right]^{1/2} \tag{4}$$

The system considered in this investigation is lightly damped, and the loading consists only of a finite band of frequencies encompassing a natural frequency of the system. For such cases, it was shown in reference 7 that equations (3) can be accurately approximated by

$$\left.\begin{aligned} \psi_o &= \overline{\sigma^2} \\ \psi_o'' &= -4\pi^2 f_o^2 \overline{\sigma^2} \\ \psi_o'''' &= 16\pi^4 f_o^4 \overline{\sigma^2} \end{aligned}\right\} \tag{5}$$

where f_o is the resonant frequency of the vibrating system. Substitution of equations (5) into equations (2) and (4) yields

$$\left.\begin{aligned} P_m(\sigma) &= 0 && (-\infty < \sigma < 0) \\ P_m(\sigma) &= \frac{f_o}{\overline{\sigma^2}} \sigma e^{-\frac{\sigma^2}{2\overline{\sigma^2}}} && (0 < \sigma < \infty) \end{aligned}\right\} \tag{6}$$

and

$$\sqrt{\overline{\sigma_p^2}} = \sqrt{2\overline{\sigma^2}} \tag{7}$$

Then equation (1), upon substitution of equations (6) and (7), becomes

$$T_f = \left[\frac{2f_o}{\overline{\sigma_p^2}} \int_0^{\infty} \frac{\sigma e^{-\frac{\sigma^2}{\overline{\sigma_p^2}}} \, d\sigma}{N(\sigma)} \right]^{-1} \tag{8}$$

For the configuration under consideration in this investigation (where f_o = 119 cps), equation (8), upon substitution of values of $N(\sigma)$ from the average SN curve of figure 10, is integrated numerically for the probable time to failure for various values of $\sqrt{\overline{\sigma_p{}^2}}$. (The method of calculation differs from that presented in reference 7 in which an analytical approximation for $N(\sigma)$ was used in order to obtain an analytical expression for T_f in terms of an equivalent stress.) The numerical integration of equation (8) is equivalent to the usual method of computing linear cumulative damage by Miner's method. The results giving the probable time to failure plotted against $\sqrt{\overline{\sigma_p{}^2}}$ are shown by the long and short dashed curve of figure 11.

DISCUSSION OF RESULTS

The results of the spectral analysis of the stress response of a typical specimen for the random-loading tests presented in figure 7(c) show that the specimen responds only to frequency components near its own natural frequency even though the power spectrum of the force input covered a much wider band. (See fig. 7(b).) Thus, the specimen acts as a narrow-band filter at its own natural frequency, and changing the natural frequency in the range of 50 to 200 cps in these tests would not alter appreciably the nature of the response. However, changing the natural frequency would change the frequency of stress response and thus would change the time to failure. The smooth nature of the time history of the stress and the presence of beats also indicate that the specimen responds only to a narrow band of frequency components present in the force signal. (See fig. 7(a).)

The random-loading data of figure 9 are given in terms of the root-mean-square stress, and the constant-amplitude data of figure 10 in terms of stress amplitude. In order to compare the results of figures 9 and 10 on the basis of peak stresses, which are an important quantity in fatigue life, the results of figure 9 should be expressed in terms of the root-mean-square value of peak stress by use of equation (7). It should be noted that the root-mean-square value of peak stresses for the constant-amplitude tests of figure 10 is the same as the stress amplitude. A summary of the fatigue results obtained in this investigation is given in figure 11, where the root-mean-square value of the peak nominal bending stresses, which does not include the effect of stress concentration, is plotted against time to failure. In this figure, the solid curve is obtained from the average of the random test results from figure 9, the dashed curve is the average of the constant-amplitude test results from figure 10, and the long and short dashed curve gives the theoretical calculated time to failure for random loading. In order to use the results of figure 10, it was necessary to convert the number of cycles to failure to equivalent time to failure by dividing the abscissa

of figure 10 by the natural frequency (119 cps). Comparison of the theoretical curve with the random-loading curve shows that the calculated time to failure underestimates the time to failure at the high stress levels but predicts the time to failure fairly well at the low stress levels. The discrepancy at the high stress levels may be attributed to the fact that the theory neglects the effects of residual stresses and strain-hardening produced by occasional large local stress peaks on the amount of subsequent fatigue damage. It is of interest to compare the random-loading curve with the constant-amplitude-loading curve in figure 11. Comparison at a given stress level indicates that random loading gives a shorter time to failure than constant-amplitude loading at the lower stress levels and a longer time to failure at the higher stress levels.

The types of failure obtained in the random-loading tests varied with stress level as may be seen in the photomicrographs of figure 12. Figure 12(a) shows the type of failure for a root-mean-square stress of 12,700 psi, and figure 12(b) for a root-mean-square stress of 4,760 psi. For each type of failure, it appears that the cracks originated at the corners and grew inwardly until only the cross section shown by the dark area remained at the time of final failure. The rate of crack growth was fairly slow; and in most of the specimens tested, there were indications of the initiation of cracks before half the total time to failure.

CONCLUSIONS

Fatigue tests were made for 125 notched cantilever-beam specimens of 7075-T6 aluminum alloy under a random loading. Results were also obtained for 46 similar specimens under constant-amplitude loadings. In both types of tests, only lateral forces were applied at the tip of the specimen. Comparison of the two sets of results on the basis of root-mean-square value of the peak nominal stresses indicated that random loading produces fatigue failure in the shorter time at the lower stress levels, while at the higher stress levels constant-amplitude loading produces failure in shorter time. A theoretical calculation based on Miner's cumulative damage criterion was made and compared with the results of the jet noise tests. The theoretical result showed satisfactory agreement for low values of stress but underestimates the time to failure at the higher values of stress.

Langley Research Center,
National Aeronautics and Space Administration,
Langley Field, Va., January 13, 1959.

REFERENCES

1. Press, Harry: Atmospheric Turbulence Environment With Special Reference to Continuous Turbulence. Rep. 115, AGARD, North Atlantic Treaty Organization (Paris), Apr.-May, 1957.

2. Liepmann, H. W.: On the Application of Statistical Concepts to the Buffeting Problem. Jour. Aero. Sci., Dec. 1952, pp. 793-800, 822.

3. Walls, James H., Houbolt, John C., and Press, Harry: Some Measurements and Power Spectra of Runway Roughness. NACA TN 3305, 1954.

4. Lassiter, Leslie W., Hess, Robert W., and Hubbard, Harvey H.: An Experimental Study of the Response of Simple Panels to Intense Acoustic Loading. Jour. Aero. Sci., vol. 24, no. 1, Jan. 1957, pp. 19-24, 80.

5. Lassiter, Leslie W., and Heitkotter, Robert H.: Some Measurements of Noise From Three Solid-Fuel Rocket Engines. NACA TN 3316, 1954.

6. Hess, Robert W., Fralich, Robert W., and Hubbard, Harvey H.: Studies of Structural Failure Due to Acoustic Loading. NACA TN 4050, 1957.

7. Miles, John W.: An Approach to the Buffeting of Aircraft Structures by Jets. Rep. No. SM-14795, Douglas Aircraft Co., Inc., June 1953.

8. Miner, Milton A.: Cumulative Damage in Fatigue. Jour. Appl. Mech., vol. 12, no. 3, Sept. 1945, pp. A-159 - A-164.

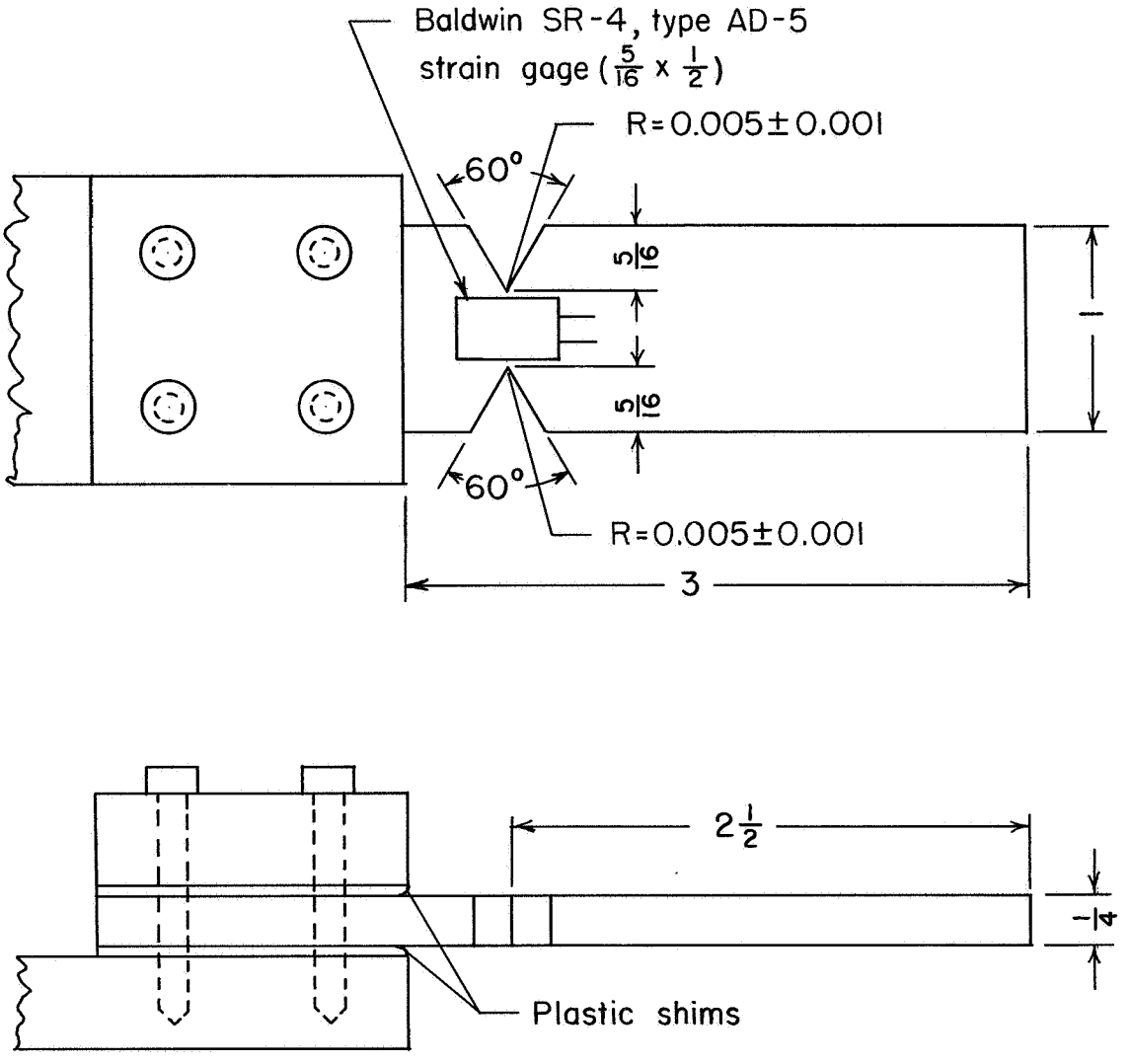

Figure 1.- Test specimen. All dimensions are in inches.

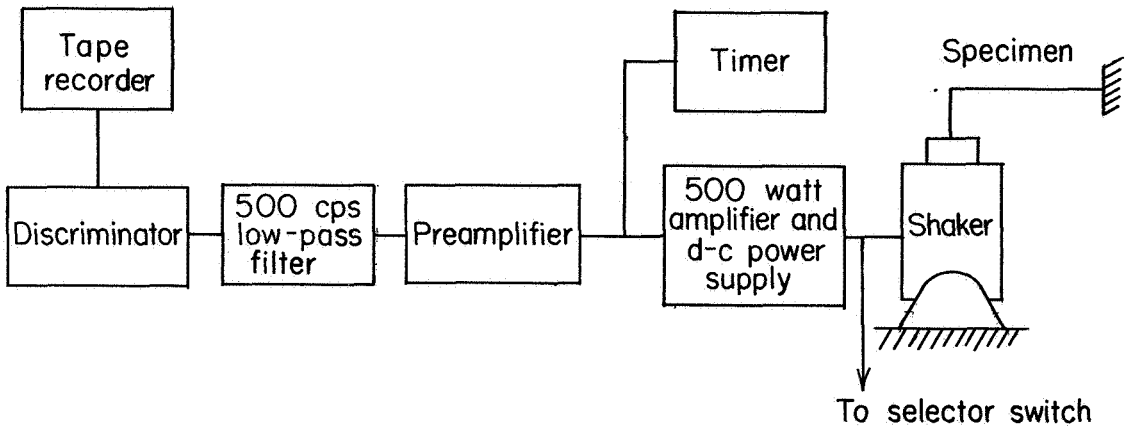

(a) Force-application equipment.

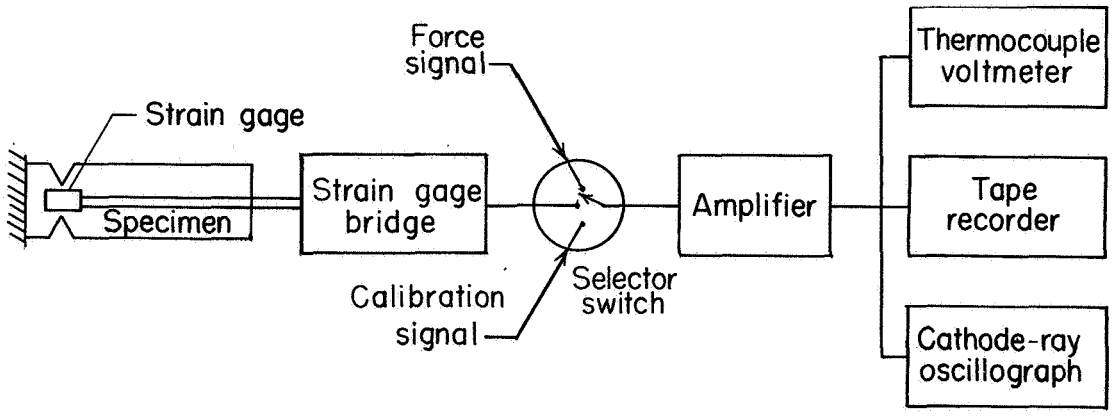

(b) Data-measuring equipment.

Figure 2.- Schematic diagram of test equipment.

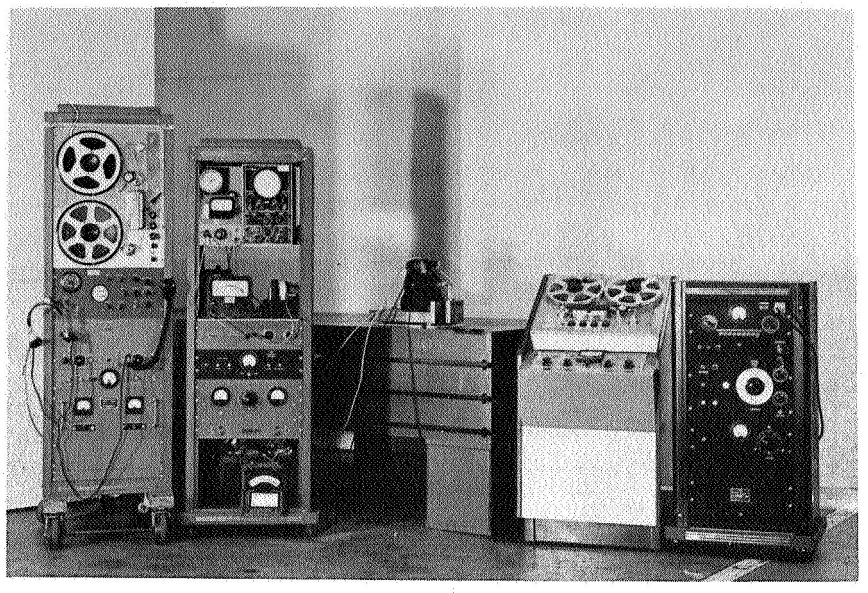

Figure 3.- Random-loading equipment. L-57-4372

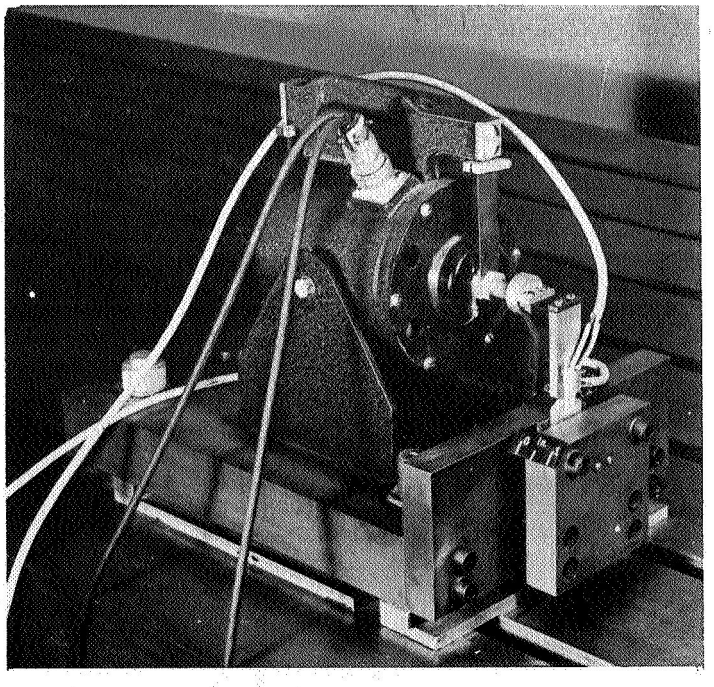

L-57-4373
Figure 4.- Specimen mounted in shaker for random-loading tests.

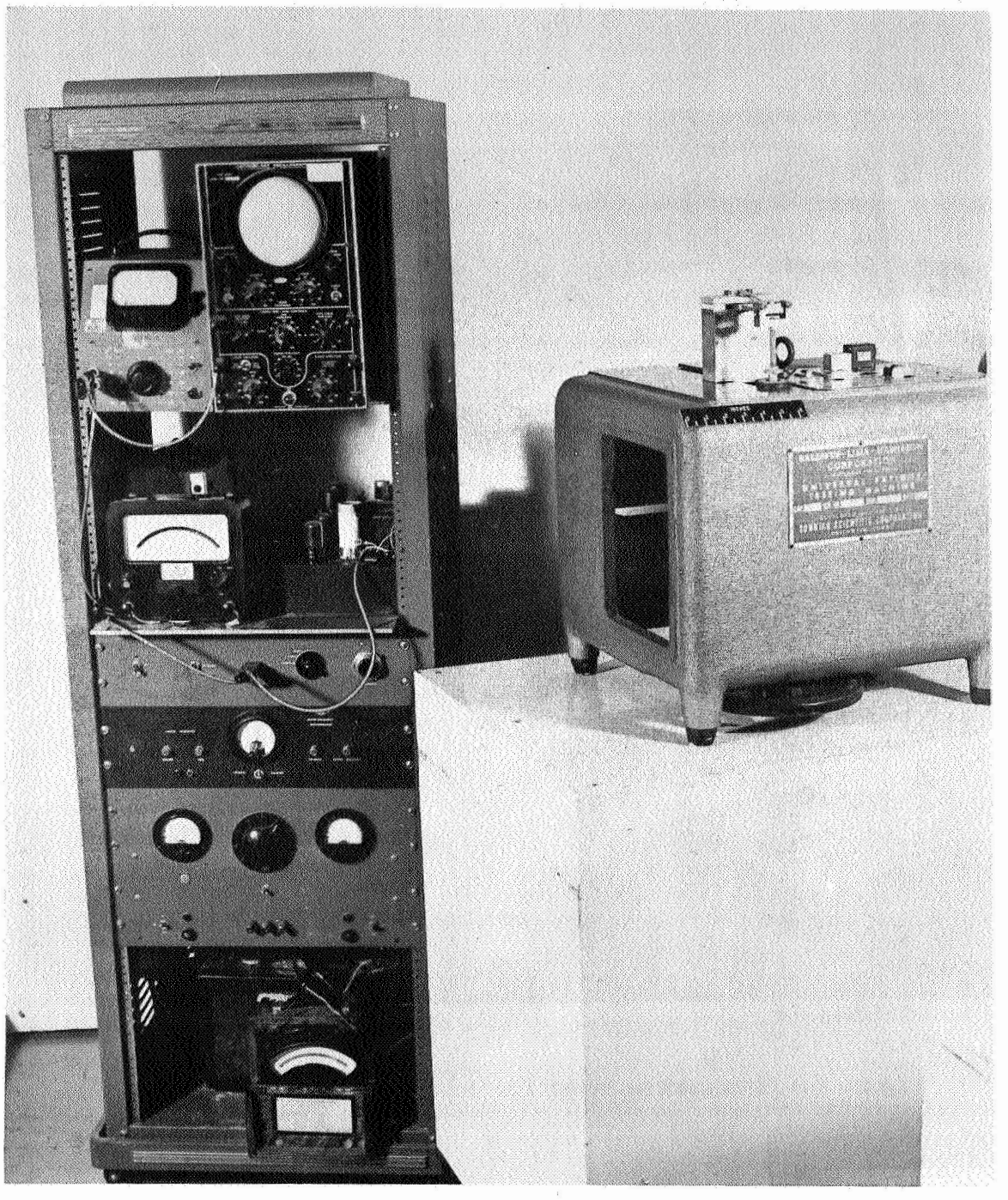

Figure 5.- Constant-amplitude loading equipment. L-57-4374

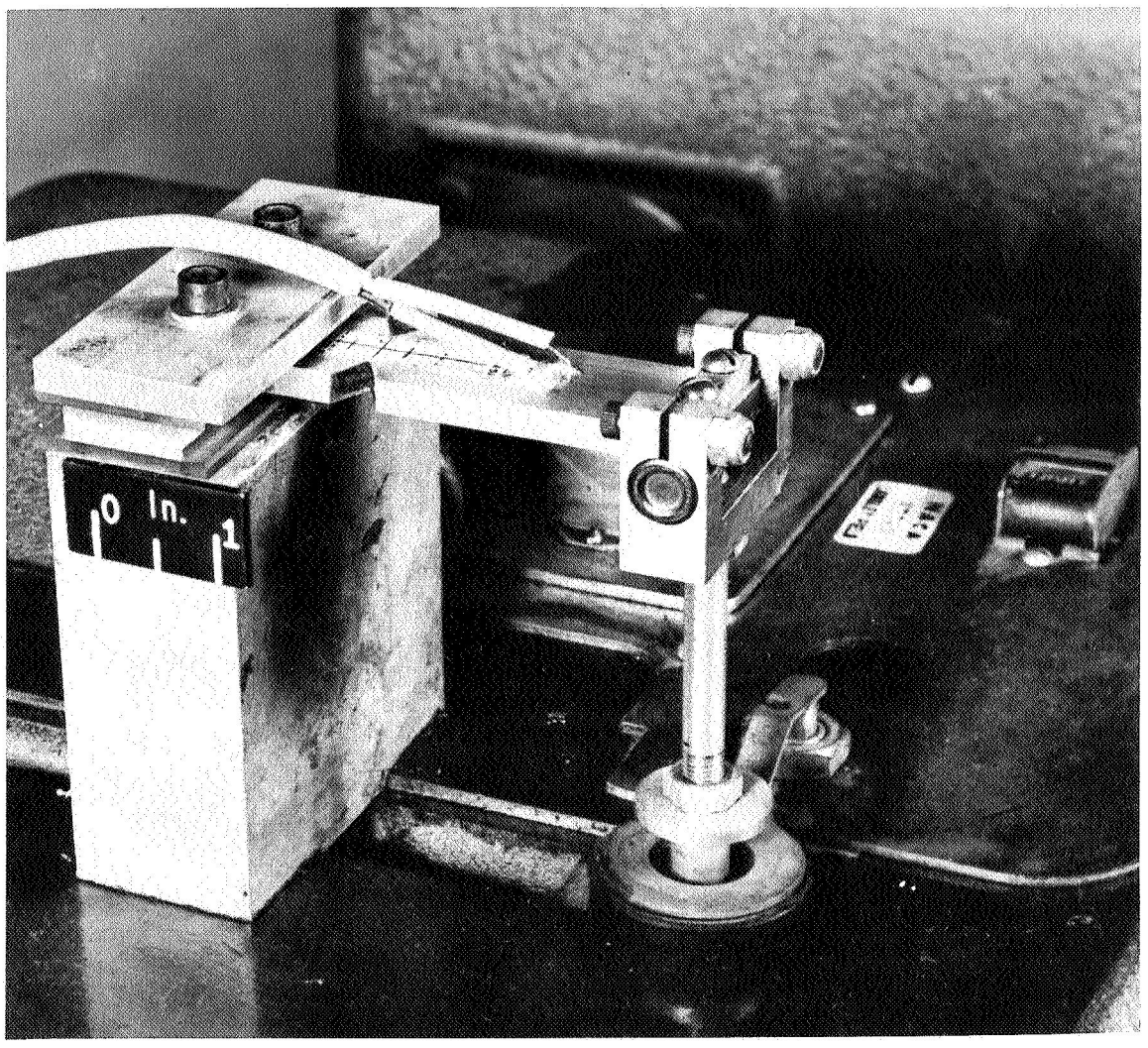

L-57-4376

Figure 6.- Specimen mounted for constant-amplitude tests.

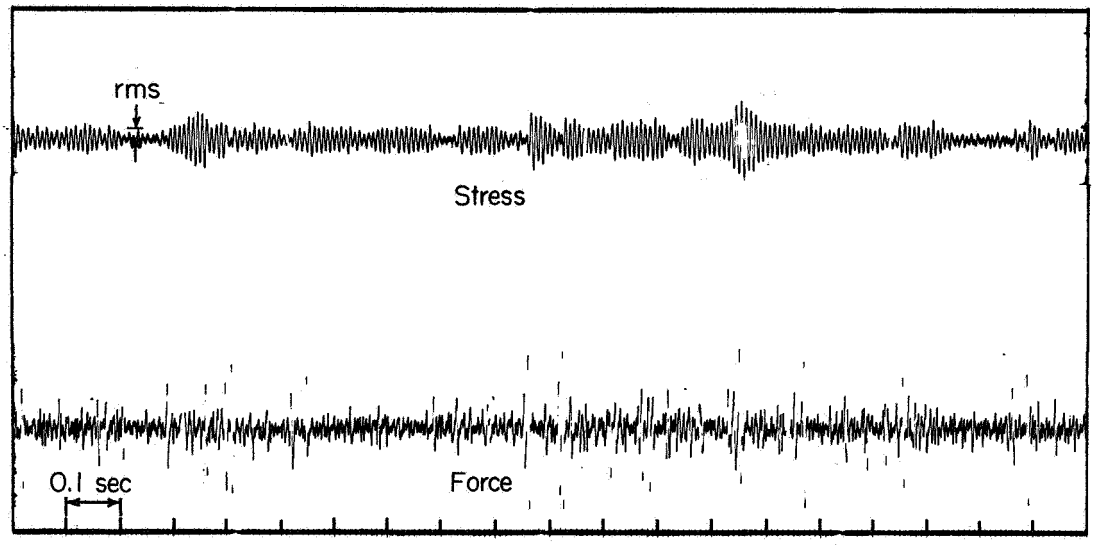

(a) Time histories of force input and stress output.

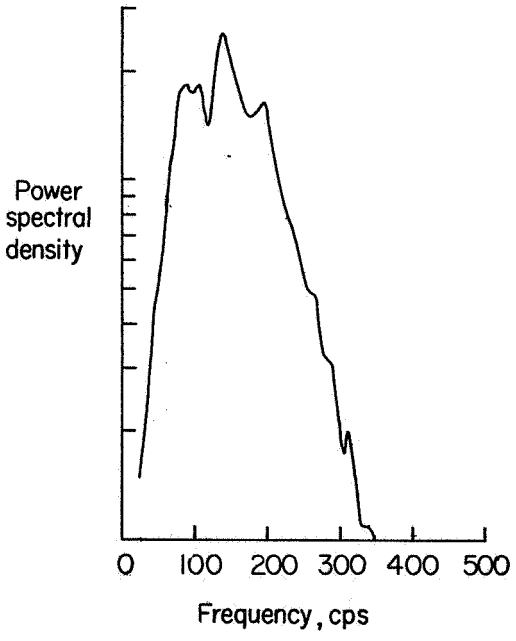

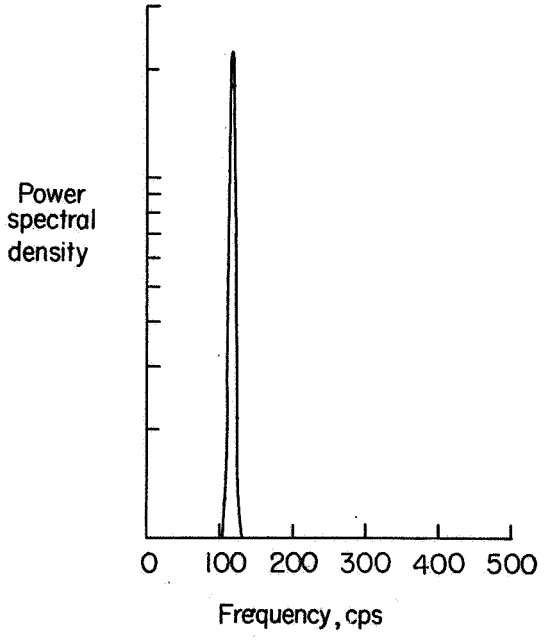

(b) Power spectrum of force input. (c) Power spectrum of stress output.

Figure 7.- Random-loading characteristics of force input and stress output for typical specimen.

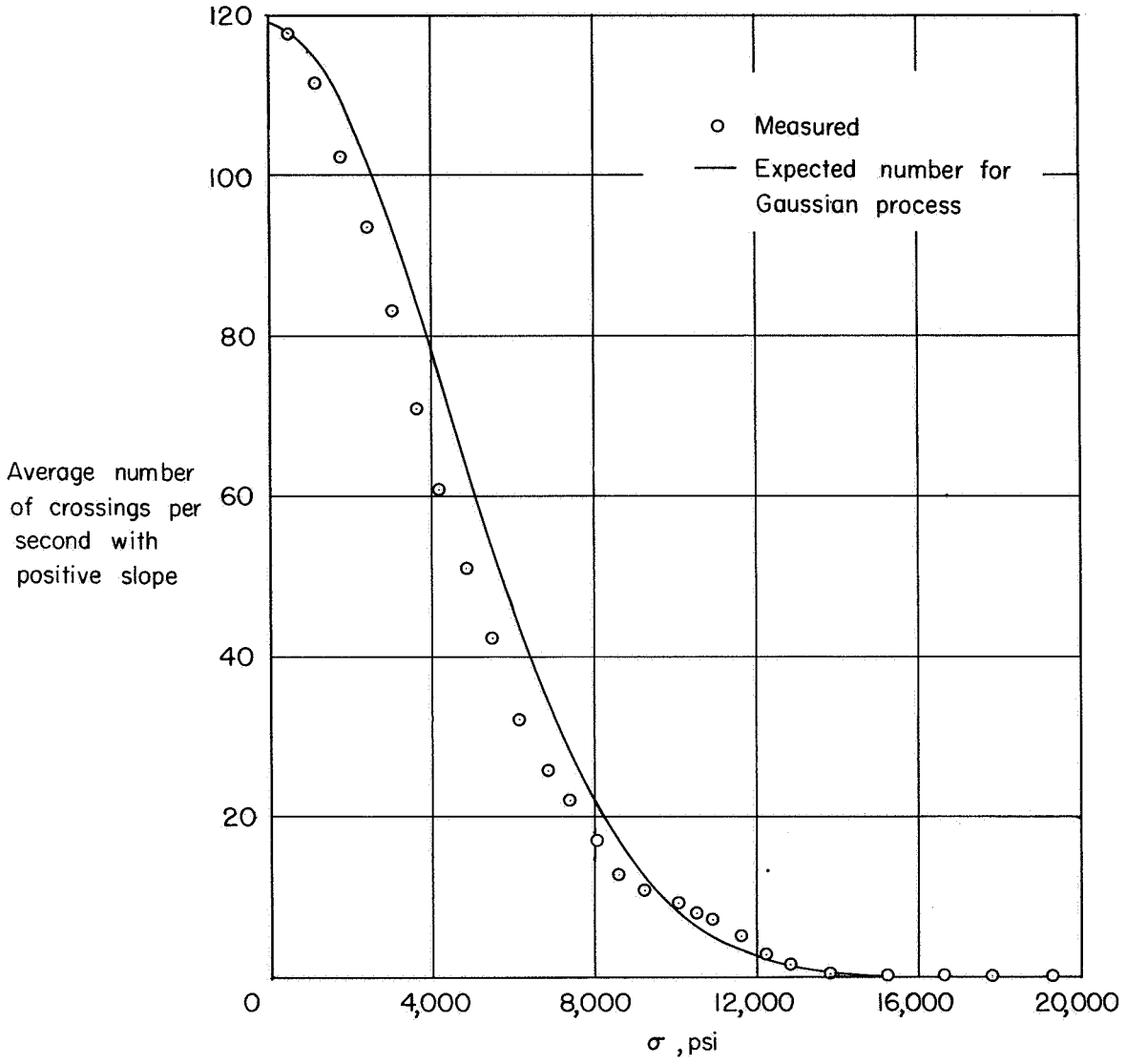

Figure 8.- Average number of crossings per second of stress level, σ, with positive slope for test with a root-mean-square stress of 4,330 psi.

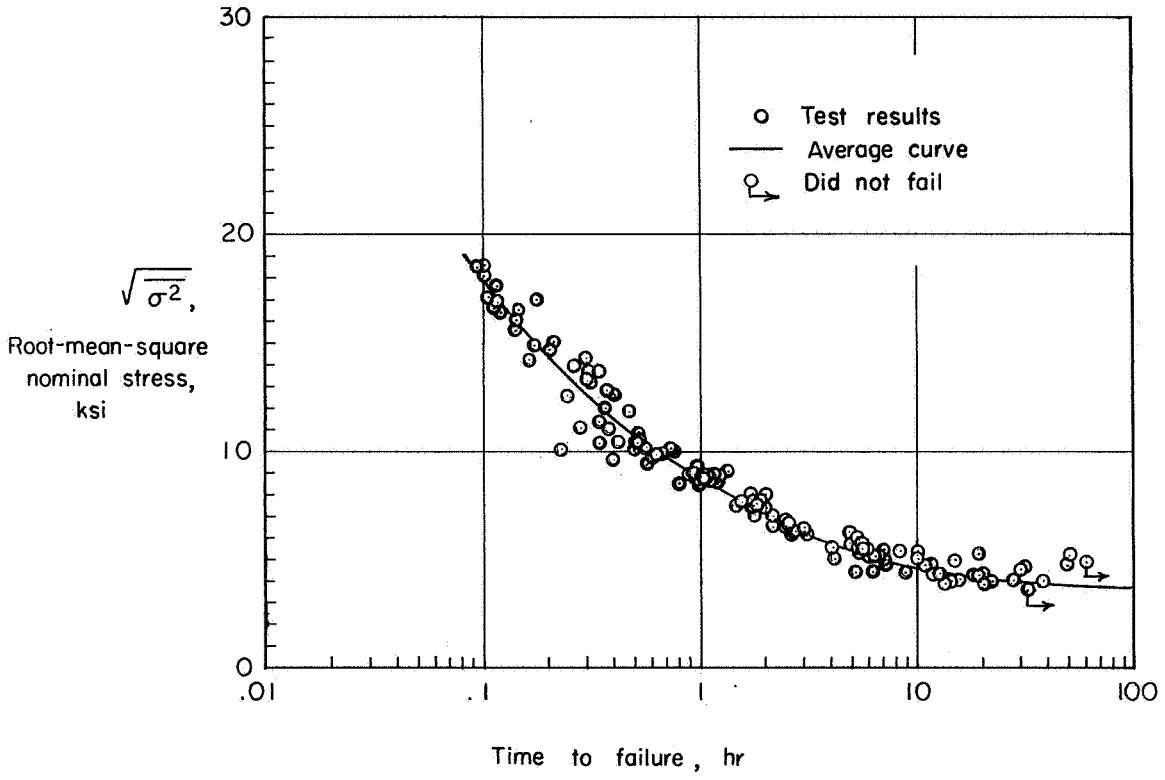

Figure 9.- Fatigue results of random-loading tests.

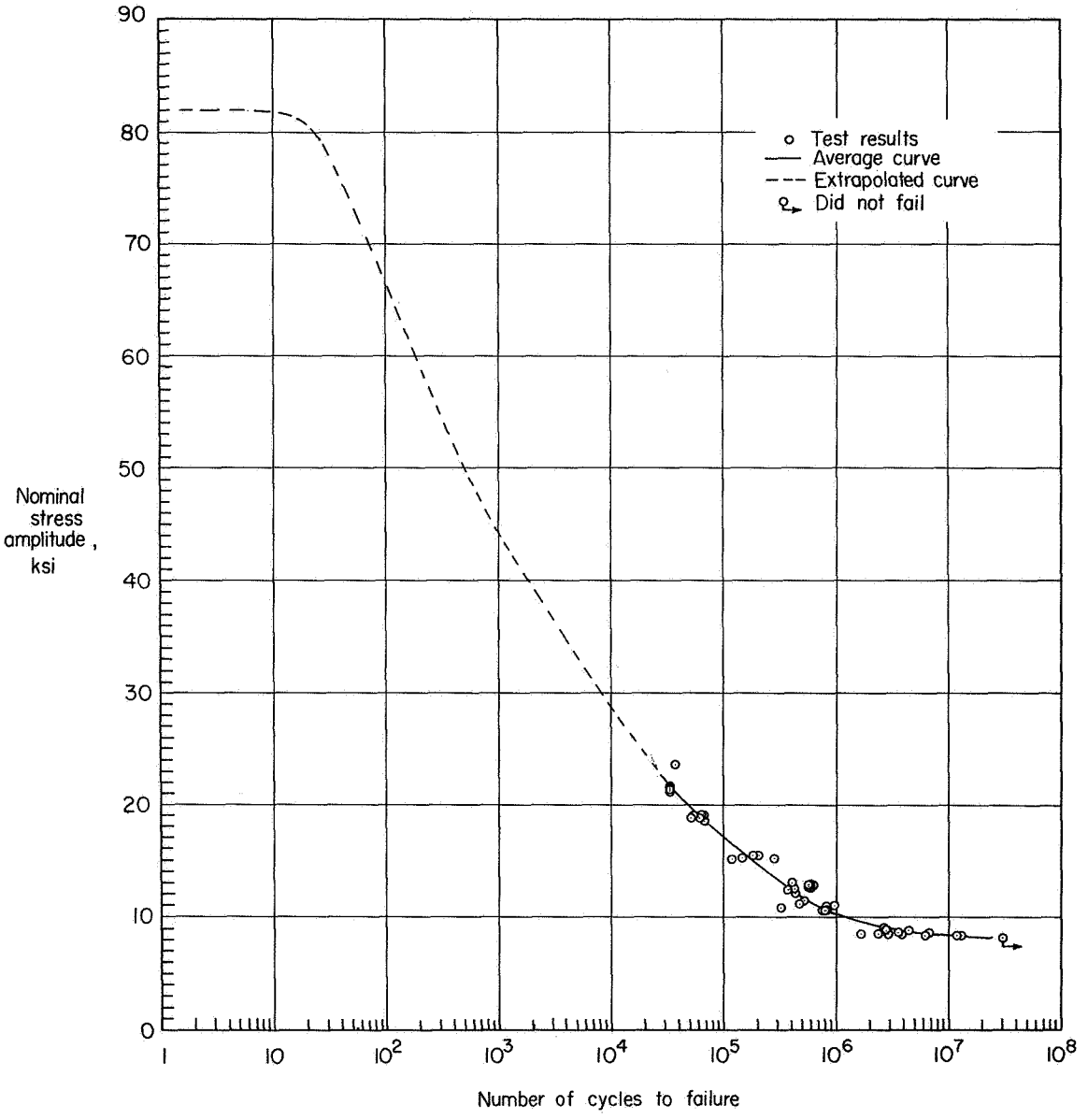

Figure 10.- Fatigue results of constant-amplitude loading tests.

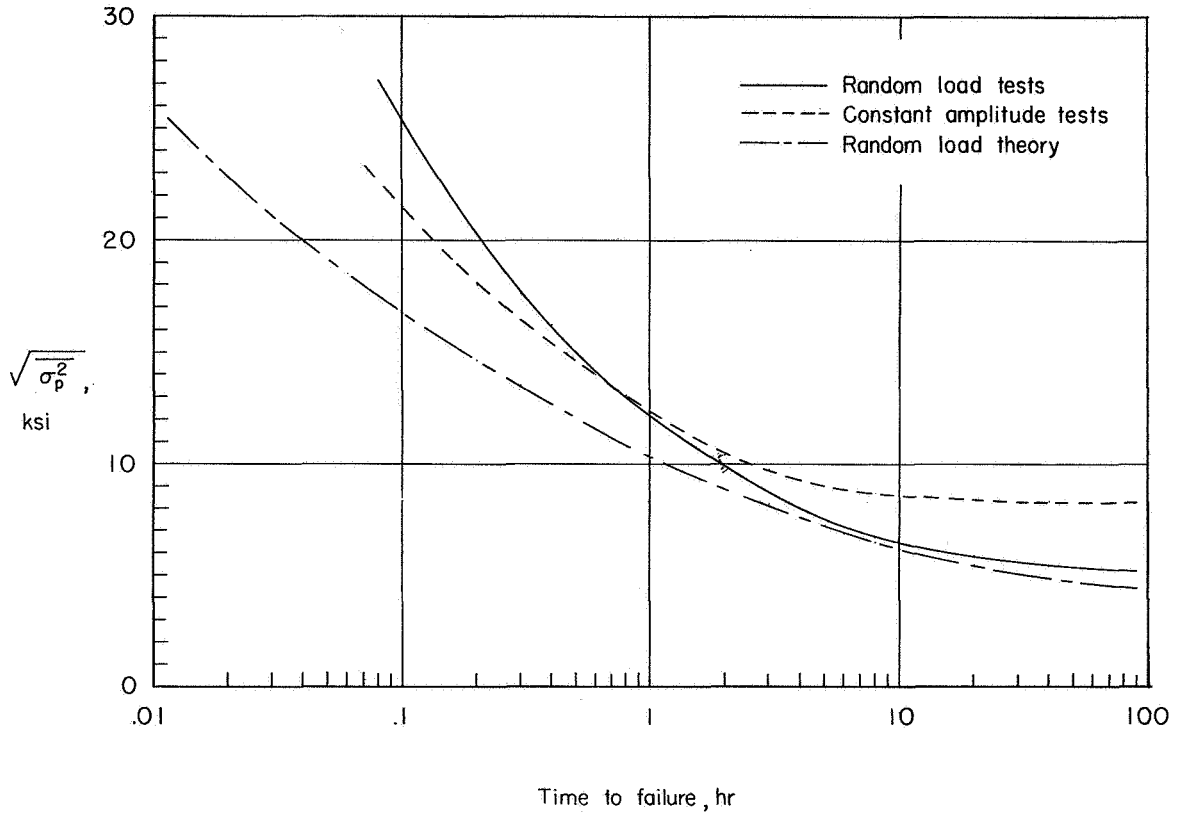

Figure 11.- Comparison of fatigue results of random-loading tests with those of constant-amplitude loading tests and with theoretical results. $\sqrt{\overline{\sigma_p{}^2}}$ = Root-mean-square value of peak nominal stress.

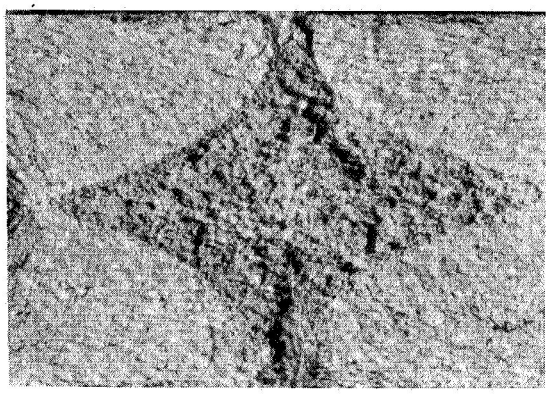

(a) $\sqrt{\overline{\sigma^2}}$ = 12,700 psi.

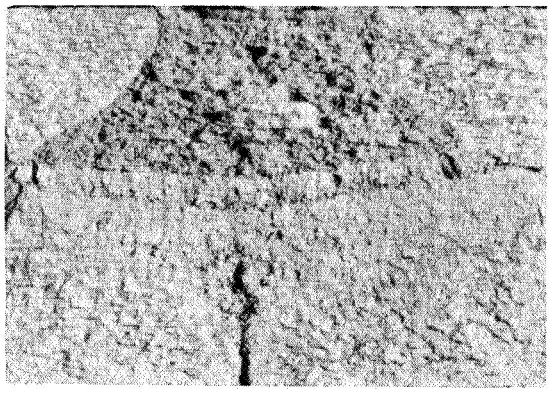

(b) $\sqrt{\overline{\sigma^2}}$ = 4,760 psi.

L-59-169

Figure 12.- Photomicrographs (×8) of typical specimen failures obtained in random-loading tests.